Calculations and Measurements of Rotating Magnetic Field Current Drive in FRCs

A.L. Hoffman, R.D. Brooks, E. Crawford, H.Y. Guo, K.E. Miller, R.D. Milroy, J.T. Slough, 1)
S. Tobin 2)
1) Redmond Plasma Physics Laboratory, University of Washington, Seattle, Washington, USA
2) Los Alamos National Laboratory, Los Alamos, New Mexico, USA
E-mail: hoffman@aa.washington.edu

Abstract. Rotating Magnetic Fields (RMF) have been demonstrated to drive currents in many rotamak experiments, but use with an FRC confined in a flux conserver imposes special constraints. The strong current drive force results in a near zero density at the separatrix, and the high average beta condition requires the current to be carried in an edge layer near the separatrix. The RMF can only penetrate into this layer by driving the azimuthal electron velocity synchronous with the RMF frequency. Build-up or maintenance of the flux throughout the FRC occurs due to the torque imposed on the electrons in this layer exceeding the total resistive torque due to electron-ion friction. Current is maintained on the inner flux surfaces by an inward radial flow. Particle balance is maintained by a swirling axial flow from inner to outer field lines. This process is seen using a new numerical code, and the resultant flux build-up and calculated profiles are demonstrated on the STX and TCS RMF FRC formation experiments.

1. Introduction

Rotating Magnetic Fields (RMF) have been calculated to drive electron currents in cylindrical plasmas [1] and flux sustainment has been demonstrated in many previous rotamak experiments [2]. The rotating field at high frequency ω can penetrate into the plasma column despite a small classical skin depth $\delta = (2\eta_{//}/\mu_o\omega)^{1/2}$ by driving the electrons into synchronous rotation ω_r so that the relative frequency seen by the electrons $\varpi = \omega - \omega_r << \omega$. The effective penetration depth $\delta^* = (2\eta_{//}/\mu_o\varpi)^{1/2}$ can then be comparable with the column radius r_s. An understanding of how RMF current drive applies to elongated FRCs in cylindrical flux conservers has recently been developed through analytical [3] and numerical [4] models where radial and axial equilibrium is imposed. Since the RMF force on the electrons must be sufficient to overcome resistive electron-ion cross-field friction, normal outward particle diffusion is also reversed, producing a near vacuum at the FRC separatrix. This minimal separatrix pressure, coupled with the high beta of an elongated FRC, results in the equilibrium azimuthal plasma current being carried in a thin layer. The thickness of the layer, Δr, where the electrons are driven to synchronous rotation by the RMF, will depend on the electron density. The RMF will not penetrate further than this layer no matter how large the driving force since generation of additional azimuthal current beyond what is necessary to reverse the external field will result in flux generation and plasma expansion. The process will reach equilibrium when the external field becomes high enough (the external flux is compressed against the flux conserver) that the RMF and frictional forces are balanced. The resultant RMF field lines are indicated by the numerical calculation shown on Fig. 1.

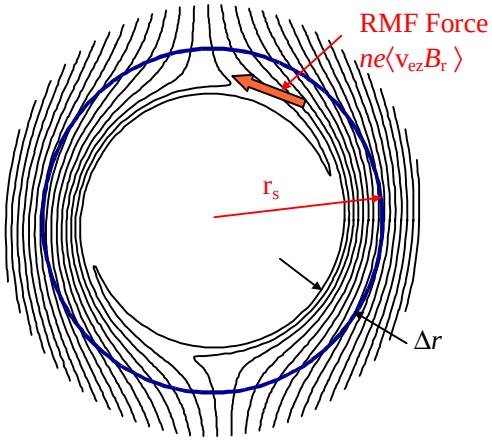

Figure 1. Numerical calculation of RMF penetration into an equilibrium FRC.

2. RMF Current Drive Theory

The RMF force on the electrons is due to the driven axial oscillation of the electrons being in-phase with the radial component of the transverse field. This can be shown at the plasma edge to be $F_\theta = ne\langle v_{ez}B_r\rangle = 2B_\omega^2/\mu_o r_s$ [3]. If this force exceeds the electron-ion friction, $F_\eta = nm_e\omega r_s\nu_\perp$, then the electrons can be accelerated to a velocity ω_r nearly equal to ω and the RMF can penetrate further than the simple skin depth δ. This condition is usually expressed by requiring the relative drive parameter $\gamma = \omega_{ce}/(\nu_{//}\nu_\perp)^{1/2}$ to exceed the skin depth parameter $\lambda = r_s/\delta$, where $\omega_{ce} = eB_\omega/m_e$ is the electron cyclotron frequency related to the rotating field strength B_ω, and $\nu_{//}$ and $\nu_\perp$ are the effective parallel and perpendicular electron collision frequencies used to represent the resistivity $\eta = m_e\nu/ne^2$. r_s is the FRC separatrix radius.

A simple model was developed in Ref. 3 to relate the build-up of flux in an FRC to the difference between total RMF and resistive torques on the electrons. This torque description is necessary since the RMF force acts only on the electrons beyond the FRC field null, but the resistive torque is due to the total FRC current. The analysis given in Ref. 3 expresses this result as

$$\left.\frac{d\phi}{dt}\right)_R = \frac{2}{ner_s^2}\left(T_M - T_\eta\right) \qquad [1]$$

where

$$T_M \approx 0.87\left(\frac{\delta^*}{r_s}\right)T_o \quad \text{with} \quad T_o = \frac{2\pi r_s^2 B_\omega^2}{\mu_o} \qquad [2]$$

and

$$T_\eta \approx 0.5\left(\frac{\lambda}{\gamma}\right)^2\left(1-\frac{\delta^*}{2r_s}\right)\left(\frac{\delta^*}{r_s}\right)T_o \ . \qquad [3]$$

In this model $\delta^* = \Delta r$ is determined by the equilibrium profile of a high beta FRC and is always less than the distance between the separatrix r_s and the field null $R = r_s/\sqrt{2}$. In the above equations γ is based on the peak density n_m. γ based on the average density in the driven layer, about $n_m/2$, must always be greater than λ.

An analytic calculation based on quasi-equilibrium, for conditions similar to those used in TCS, is shown in Fig. 2. The important parameter is the ratio of separatrix to flux conserver radius, $x_s \equiv r_s/r_c$ since the poloidal flux scales approximately as x_s^4 and the average plasma beta is $\langle\beta\rangle = 1 - \frac{1}{2}x_s^2$. (For an FRC we wish to reduce beta from its usual high value for theta pinch formed FRCs with $x_s \le 0.5$ in order to provide more confinement flux.) The analytic program, based on a continual quasi-equilibrium, cannot start from a small x_s value since the very high beta would generally be incompatible with an RMF produced profile. The analytic calculation is thus started at an arbitrary $x_s = 0.6$, which is about the minimum we would ever

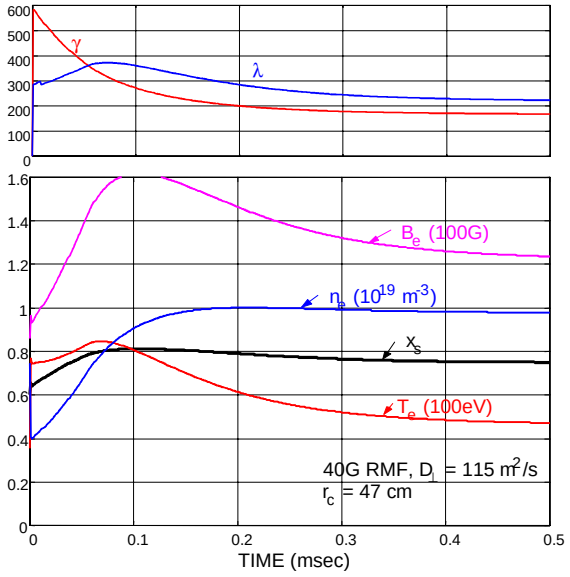

Figure 2. Numerical calculation of flux build-up for conditions appropriate to TCS experiment.

expect to see once an RMF driven FRC comes into equilibrium. The vacuum field B_o is specified as 60 G in the Fig. 2 calculation and the external field $B_e = B_o/(1-x_s^2)$ is highly compressed between the FRC separatrix and the flux conserver. The electron temperature time history was chosen to approximately mimic that seen experimentally, and is initially high before full ionization is complete. The peak density n_m is set by pressure balance, $n_m = (B_e^2 + 2B_\omega^2)/2\mu_o T_e$, where the ions are assumed cold and the radial pressure produced by the RMF field, $B_\theta \sim 2B_\omega$ at the edge, is also accounted for.

In the above calculation the parallel collisionality was assumed classical but this is irrelevant for the simple analytic calculation since only the perpendicular resistivity affects the γ/λ ratio. The perpendicular resistivity $\eta_\perp = m_e\nu_\perp/ne^2$ (with $D_\perp = \eta_\perp/\mu_o$) was set at a fixed value. The only thing that then limits continual flux build-up and expansion of the FRC is the rise in electron density, which increases the frictional drag and lowers the ratio of γ/λ. The FRC expansion initially reaches a value $x_s = 0.83$, but then decreases to a new equilibrium due to completion of ionization, reduction in temperature, and the resultant increase in electron density.

3. Experiments in STX and TCS

The TCS (Translation, Sustainment, and Confinement) experiment was built primarily to develop the ability to build up the flux of an FRC formed by normal field reversed theta-pinch (FRTP) techniques. In this way the high powers required to overcome initial radiation and ionization barriers encountered in high beta plasmas could be supplied by the theta-pinch implosion. TCS has an 80-cm diameter by 2.5-m long quartz plasma chamber with quasi-steady axial field coils and RMF antennas. FRCs are formed in the old LSX/mod (now 40-cm diameter) facility [5,6] and translated and expanded into TCS. In this way hot ion plasmas can be trapped at the lower densities appropriate to RMF drive (and to steady-state reactors). Only some initial exploratory work has so far been conducted in this manner. Most experiments to-date have been carried out using LSX/mod as a preionization source, and generating FRCs in TCS from an initial gas fill. The same type of FRCs have been formed in the 40-cm diameter STX device [7] where detailed internal field measurements have been made. FRCs formed in this manner have had relatively low densities, $n_m \sim 10^{19}$ m^{-3} and temperatures, $T_e \leq 100$ eV with cold ions. Attempts will be made in the future to increase these values through better preionization, impurity control, and initially higher power RMF.

Measurements of the excluded flux, $\Delta\phi = \pi r_s^2 B_e$, the external field B_e, the internal field B_{int} at r = 15 cm, the double pass integrated line density across the FRC diameter, and the RMF antenna current are shown on Fig. 3 for RMF start-up in TCS. The excluded flux rapidly builds up to about 8 mWb, but then decreases somewhat as the electron density increases to about 10^{19} m^{-3}. The flux conserver radius is 47 cm so that the final separatrix radius of 35 cm, about 5 cm inside the quartz plasma tube wall, corresponds to an x_s ratio of 0.75. The RMF antennas are located at a radius of about 54 cm, and produce a rotating field of strength B_ω(G) = 6.4I_{ant}(kA), or approximately 35 G for the displayed shot.

The initial data shown for TCS was taken without any discharge cleaning and the impurity level was fairly high. The data shown on Fig. 3 had the highest inferred resistivity of any shot yet taken, and illustrates the ability to achieve steady-state conditions under even such extreme conditions. The normal particle confinement time for such an FRCs would be under 50 μsec, yet

the total particle inventory remains approximately constant for the full duration of the RMF application.

The data shown on Fig. 3 shows all the features of the Fig. 2 analytic calculation, with the FRC radius achieving a high value, and then decreasing slightly as the electron density rises and the electron-ion friction increases. The value of $\eta_\perp$ used in the calculation also agrees fairly well with that inferred from the decay of the FRC, $\tau_\varphi = r_s^2/16D_\perp$, after the RMF is turned off, and with the measured absorbed RMF power (~2 MW). This tends to confirm the basic tenets of our quasi 1-D model. Future TCS work will involve improving the vacuum cleanliness, working with lower resistivity FRCs, and measuring temperature profiles, ion velocities, and radiation loss powers.

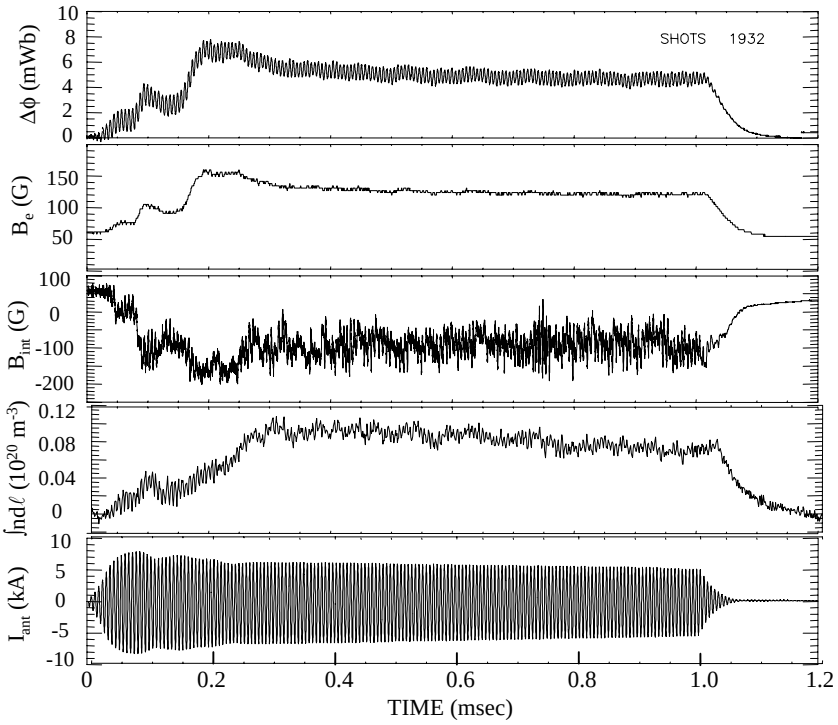

Figure 3. Experimental data for an RMF formed FRC in the TCS

Detailed internal field measurements of both B_z and the RMF B_θ have been made in the smaller, 40-cm diameter, STX device. Radial profiles are shown on Fig. 4 along with the density inferred from pressure balance $n = (B_e^2 + 0.5B_\theta^2 - B_z^2)/2\mu_o T$ with T chosen to give a best fit to the relationship $-j_\theta = (dB_z/dr)/\mu_o = ne\omega r$ near the column edge. The density profile inferred in this way from the measured current is in excellent agreement with the pressure balance density over the region in which the RMF penetrates, giving support to the inference of synchronous rotation. The profile is different from the normal non-RMF driven FRC rigid rotor (RR) profile with rigid rotation everywhere, since those profiles have high pressures at the separatrix. The inferred density at the separatrix in the Fig. 4 data appears to be near zero, although this is somewhat clouded by the separatrix radius in the STX experiments usually being very close to, or beyond, the inner wall of the quartz plasma tube.

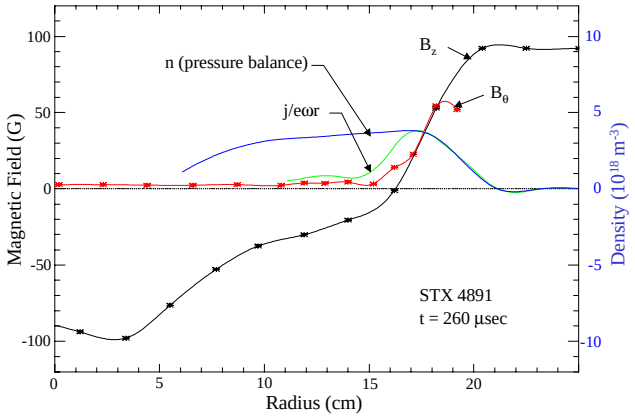

Figure 4. Comparison of pressure balance density (T = 55 eV) with density inferred from n = -j/eωr.

The mechanism whereby the separatrix density is reduced to near zero, and the RMF force maintains the current over the entire profile, is illustrated by the 1-½D (1-D radial plus pressure equilibration on flux 'surfaces' with implied axial contraction or expansion to satisfy the average beta constraint) MHD calculation shown on Fig. 5. An inward radial velocity is calculated on both sides of the field null, which is stipulated to be sustained by a swirling axial flow from inner to outer field lines to maintain pressure balance on flux surfaces.

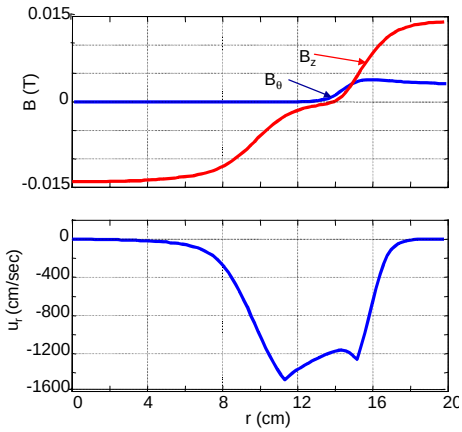

Figure 5. Calculated magnetic field and radial flow velocities for STX

The generalized Ohm's Law in the theta direction can be written as

$$E_\theta = \eta_\perp j_\theta + v_r B_z + \langle j_z B_r \rangle / ne . \qquad [4]$$

The bracketed term is the RMF current drive term, where j_z is the axial electron current induced by the applied RMF. Since in steady-state the azimuthal electric field must be zero everywhere, the radial 'diffusive' velocity will be

$$v_r = \frac{1}{B_z}\{(-\eta_\perp j_\theta) - \langle v_{ez} B_r \rangle\} . \qquad [5]$$

Inside the field null ($B_z < 0$) where the RMF doesn't penetrate, the inward v_r just balances resistivity so that $E_\theta = 0$, while outside the field null ($B_z > 0$) the RMF drive must be strong enough to not only compensate for resistivity, but also reverse the normally outward diffusion. This has the consequence of essentially eliminating particle loss, which is not always beneficial since it makes impurity and density control difficult.

Another feature of RMF current drive in FRCs is the production of a strong 'pondermotive' force gradient in the outer edge. The radial pressure gradient can be calculated approximately as

$$\frac{dp}{dr} = j_\theta B_z + \langle -j_z B_\theta \rangle = \nabla \left\{ \frac{B_z^2}{2\mu_o} + \frac{B_\theta^2}{4\mu_o} \right\} . \qquad [6]$$

This force gradient can be highly stabilizing, and no instabilities have been seen in the RMF driven FRCs, except for sometimes a slight m=1 wobble, even though the ions are cold and should be in a very MHD-like regime.

Measurements of the internal confinement field B_z and the RMF B_θ in STX are shown on Fig. 6 at various times. The RMF was applied at 50 μsec to an ionized plasma column in a 90 G magnetic field. The axial field was reversed on axis by 150 μsec, leading to formation of an FRC and exclusion of the RMF from inside the field null. The internal flux is then built up to about 0.35 mWb. The inferred resistivity for this shot, both from the maximum flux achieved and the decay rate after RMF shutoff is about 60 μΩ-m. The absorbed RMF power appeared very low (~50 kW), characteristic of an inferred cross-field resistivity under 20 μΩ-m [5], but power absorbed in circuit resistances was so much higher it was difficult to accurately determine the portion of the RMF power absorbed by the plasma.

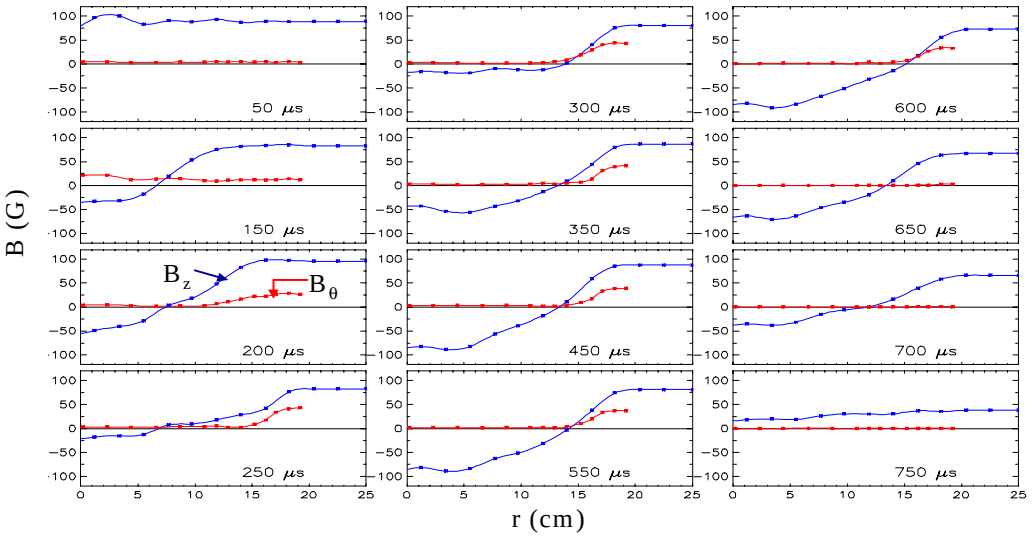

Fig 6. Internal axial field, B_z and RMF field, B_θ measurements in the STX device.

As mentioned earlier, TCS was designed to apply RMF to FRCs that were translated from the old LSX/mod device. This has only been attempted so far with very weak RMF fields. Some preliminary data is shown on Fig. 7 where excluded flux time histories are compared for injected FRCs (arriving at the TCS chamber at about 40 μsec) with and without RMF applied. The initial plasma density was about 2×10^{19} m^{-3} in a 0.2 kG field, but it rose rapidly in the RMF driven case, producing conditions well beyond what could be driven by the applied RMF field strength. The RMF antenna current is strongly reduced due to the loading produced by the plasma. Although the RMF is not strong enough to maintain the FRC flux, it does seem to maintain the total particle inventory. Experiments will be continued with stronger RMF fields, and hopefully better control of the surrounding gas inventory.

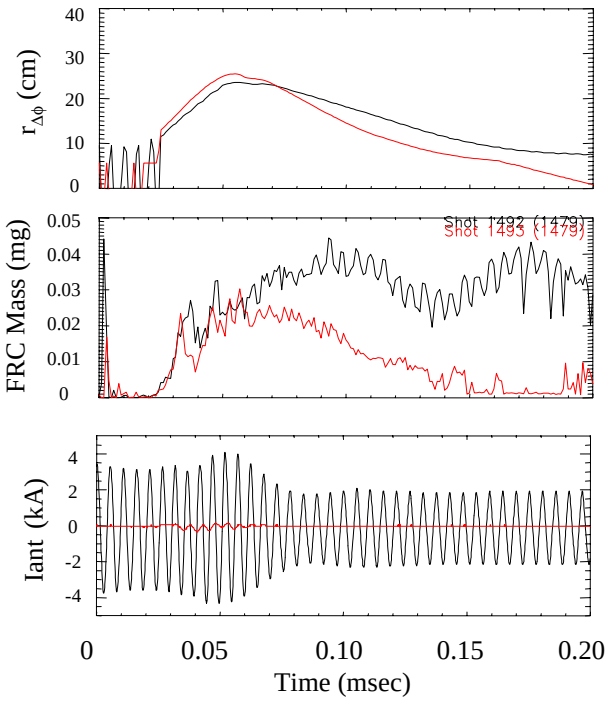

Figure 7. Initial data from RMF applied to translated TCS FRC. Black curve – with RMF, red curves – no RMF.

The ability to build up and maintain FRC flux under given conditions depends almost wholly on the degree of cross-field resistivity that it must overcome. This resistivity is certainly anomalous, with a scaling from previous high density FRC experiments [8] given by

$$D_{\perp emp} = \frac{\eta_\perp}{\mu_o} = \frac{11.2\ (\mathrm{m^2/s})}{x_s^{1/2} r_s^{0.14}(\mathrm{m}) n^{1/2}(10^{20}\,\mathrm{m^{-3}})} \approx \frac{15\ (\mathrm{m^2/s})}{n^{1/2}(10^{20}\,\mathrm{m^{-3}})}\ . \qquad [7]$$

Somewhat lower values have been measured at lower densities (although not in preliminary TCS experiments, where impurities may be a problem), so using a value of $D_\perp = fD_{\perp\mathrm{emp}}$ the ratio of γ/λ can be written

$$\frac{\gamma}{\lambda} = \frac{0.0071\ B_\omega(\mathrm{G})}{n_m D_\perp^{1/2}(\mathrm{m^2/s})\left(\omega r_s^2\right)^{1/2}} = \frac{1}{\sqrt{f}} \frac{0.0036\ B_\omega(\mathrm{G})}{n_\mathrm{m}^{3/4}\left(\omega r_s^2\right)^{1/2}} \qquad [8]$$

where n_m has units of 10^{20} $\mathrm{m^{-3}}$, ω units of 10^6 $\mathrm{s^{-1}}$, and r_s units of m. In order for the RMF to penetrate close to the field null, the parameter (ωr_s^2) must be chosen such that the synchronous line current $I'_\mathrm{sync} = 0.5\langle n\rangle e\omega r_\mathrm{s}^2$ is not too much larger (and definitely not smaller) than the equilibrium current $I' = \Delta B_\mathrm{e}/\mu_\mathrm{o}$ with $\Delta B_\mathrm{e} = 2B_\mathrm{e}$ for the zero separatrix pressure RMF driven FRCs. If we assume that the RMF frequency is chosen correctly so that $I'_\mathrm{sync} \approx 2I'$ and $(\omega r_\mathrm{s}^2) = 0.033 B_\mathrm{e}(\mathrm{kG})/n_\mathrm{m}$, then, assuming pressure balance, the following scaling is obtained.

$$\frac{\gamma}{\lambda} = \frac{1}{\sqrt{f}} \frac{0.02\ B_\omega(\mathrm{G})}{n_m^{1/4}(10^{20})\, B_e^{1/2}(\mathrm{kG})} = \frac{1}{\sqrt{f}} \frac{0.012\ B_\omega(\mathrm{G})}{n_m^{1/2}(10^{20})\, T_i^{1/4}(\mathrm{keV})} \qquad [9]$$

The key parameter in determining the ultimate effectiveness of RMF current drive, as mentioned earlier, is the value of anomalous resistivity as represented by *f*. There is some evidence from STX that the anomalous resistivity is lowered in the region where the RMF penetrates, leading to lower absorbed power, but the empirical value of $D_\perp$, hopefully with *f* somewhat less than unity, still seems to govern the basic penetration requirements. This would lead to more of a technological problem than one of power balance, since high antenna voltages are required to produce high antenna currents and high RMF fields. Energy confinement times, as inferred from steady-state STX conditions and RMF power absorption measurements, are several times higher than extrapolated from previous scaling laws.

4. Summary & Conclusions

The measurements to-date have shown that the RMF driven FRC is a very different entity than the simple theta-pinch formed FRC. It can be truly steady-state, with very low separatrix pressure and very low particle losses. However, matters such as neutral particle surrounding pressure, which were irrelevant to previous high loss pulsed FRCs, will now be critical. There is also the matter of ion spin-up, which has not been addressed here, but will probably have to be countered by neutral beam injection in the opposite direction. Nevertheless, the promise of a new type of simple, steady-state confinement scheme is very intriguing.

Acknowledgements

The authors would like to acknowledge the participation of Sam Cohen in the STX experiments, and the contributions of Dan Lotz, Bill Reese, Lou Shrank, and Glen Wurden in building and bringing on-line the LANL built RMF power supply. Thanks are also due to Scott Kimball, Mark Kostora, and John Hayward for building the STX and TCS facilities. This work was supported by the U.S. Department of Energy.

References

[1] JONES, I.R. & HUGRASS, W.N., "Steady-state solutions for the penetration of a rotating magnetic field into a plasma column", J. Plasma Physics **26**, (1981) 441.

[2] EURIPIDES, P.E., JONES, I.R., DENG, C., "Rotamak discharges in a 0.5 m diameter spherical device", Nucl. Fusion **37**, (1997) 1505

[3] HOFFMAN, A.L., "Rotating Magnetic Field current drive of FRCs subject to equilibrium constraints", to be published in Nuclear Fusion.

[4] MILROY, R.D., "A magnetohydrodynamic model of rotating magnetic field current drive in a field-reversed configuration" to be published in Physics of Plasmas.

[5] HOFFMAN, A.L., et. al., The Large s FRC Experiment (LSX)", Fusion Technology **25**, (1995) 25.

[6] HOFFMAN, A.L., et. al., "Inductive field-reversed configuration accelerator for tokamak fueling", Fusion Technology **36**, (1999) 109.

[7] SLOUGH, J.T., & MILLER, K.E., "Flux generation and sustainment of a field-reversed configuration with rotating magnetic field current drive", Phys. Plasmas **7**, (2000) 1945.

[8] HOFFMAN, A.L. & SLOUGH, J.T., "FRC lifetime scaling based on measurements for the Large s Experiment (LSX)", Nucl. Fusion **33**, (1993) 27.